ResearchGate

See discussions, stats, and author profiles for this publication at: https://www.researchgate.net/publication/231653708

Polydiacetylene-Functionalized Noble Metal Nanocages

ARTICLE *in* THE JOURNAL OF PHYSICAL CHEMISTRY C · NOVEMBER 2009

Impact Factor: 4.77 · DOI: 10.1021/jp905787h

CITATIONS
22

READS
44

9 AUTHORS, INCLUDING:

Anna Demartini
Università degli Studi di Genova
18 PUBLICATIONS **103** CITATIONS
SEE PROFILE

Giovanna Dellepiane
Università degli Studi di Genova
213 PUBLICATIONS **2,001** CITATIONS
SEE PROFILE

Emilia Giorgetti
Italian National Research Council
137 PUBLICATIONS **809** CITATIONS
SEE PROFILE

Maurizio Muniz-Miranda
University of Florence
203 PUBLICATIONS **2,087** CITATIONS
SEE PROFILE

Available from: Maurizio Muniz-Miranda
Retrieved on: 30 January 2016

Polydiacetylene-Functionalized Noble Metal Nanocages

Anna Demartini,[†] Marina Alloisio,*[,†] Carla Cuniberti,[†] Giovanna Dellepiane,[†] Sushilkumar A. Jadhav,[†] Sergio Thea,[†] Emilia Giorgetti,[‡] Cristina Gellini,[§] and Maurizio Muniz-Miranda[||]

INSTM and Dipartimento di Chimica e Chimica Industriale, Università di Genova, Via Dodecaneso 31 - 16146 Genova, Italy, INSTM and Istituto dei Sistemi Complessi - CNR, Via Madonna del Piano 10 - 50019 Sesto Fiorentino, Firenze, Italy, Dipartimento di Chimica, Università di Firenze, Via della Lastruccia 3 - 50019 Sesto Fiorentino, Firenze, Italy, and INSTM and Dipartimento di Chimica, Università di Firenze, Via della Lastruccia 3 - 50019 Sesto Fiorentino, Firenze, Italy

Received: June 19, 2009; Revised Manuscript Received: September 14, 2009

Stable chitosan-protected noble metal nanocages of relatively small size (~50 nm) were successfully synthesized by the galvanic replacement reaction between the corresponding silver nanoparticles and $HAuCl_4$ in aqueous suspension. A broad surface plasmon band peaked around 700 nm and extended to the near-infrared was observed by properly changing the experimental conditions. To test the performance, the nanocages were functionalized with 10,12-pentacosadiynoic acid (PCDA) chains and then irradiated with UV light to induce monomer polymerization. A very high polymer conversion was observed. The time evolution of the electronic absorption and Raman spectra showed a variety of polydiacetylenic forms, including the unusual highly delocalized bluish-green phase. The nanocages act as surface-enhanced Raman scattering (SERS) active substrates with all our available excitation lines and show improved Raman activity in comparison with data from both silver and gold colloids. The shift of the plasmonic band to the NIR is expected to magnify the nonlinear response of polydiacetylene in this region.

Introduction

Size- and shape-defined metal nanoparticles are currently intensively studied for their relevant applications in technological, biological, and medical fields.[1−3] The choice of the metal type and particle shape and the control of size monodispersity are important because of the strong dependence of particle behavior on these properties. The strong plasmon absorption bands observed for metal nanoparticles, arising from the coherent oscillation of the conduction band electrons induced by the interacting electromagnetic field and known as surface plasmon resonance (SPR) bands have frequencies tunable with the particle's size and shape,[4,5] dielectric properties of the external medium and surface patterning with chemical groups for optical and biological applications.[6−9] For instance, gold or silver nanorods show an additional SPR band, which is associated to the longitudinal plasmon mode and is red-shifted by an amount depending on their aspect ratios.[7] A similar behavior is displayed also by gold nanoshells grown on the surface of silica spheres, which show a shift of the longitudinal SPR peak by varying the diameter of the SiO_2 nanoparticle and the gold shell thickness.[9,10] Moreover, further processing metal nanostructures into ones with hollow interiors, so obtaining nanocages (NCs), is expected to improve their performance in comparison with the solid counterparts because of NCs lower density and higher surface-to-volume ratio.[11−15] Recently, it has been shown that galvanic replacement reactions are a simple and convenient route to obtain hollow/porous metal[16,17] and metal alloy[18,19] nanostructures in aqueous[17−20] and organic[21] environments.

In a typical procedure, preformed metal nanostructures are kept in contact with the salt of another metal with a higher electrochemical potential, so determining a spontaneous replacement reaction in which simultaneously the first metal dissolves into ions while the second metal ions convert into atoms. The sacrificial nanostructures also act as template for the epitaxial deposition of the newly reduced metal component. On this basis, nanoshells of controllable geometric shape with hollow interiors, smooth surfaces and highly crystalline walls consisting of Ag−Au alloy could be routinely produced by titrating preexisting silver nanocores with $HAuCl_4$ in aqueous solution.[17,22,23] Compared with their solid counterparts, these metal nanocages have the following advantages:

- the SPR peak can be conveniently tuned to cover the entire spectral region from 500 to 1200 nm by simply controlling the synthesis conditions;
- small sized NCs (<50 nm), still exhibiting resonance peaks in the NIR region with high absorption coefficients, can be obtained;
- the surface can be easily passivated and/or bioconjugated by taking advantage of the well-established monolayer chemistry.

The shift of the plasmon peak of NCs to the NIR has many implications in the following fields:

- Nanomedicine and nanobiology: by tuning the NCs resonance to the 650−900 nm spectral region, where blood and tissue are radiation transparent and photons can harmlessly pass through soft biological tissues, a variety of biomedical applications are enabled, including photothermal cancer therapy, photothermally triggered drug releasing, and contrast-enhanced imaging.[23]

* To whom correspondence should be addressed. Phone: +39 010 353 8714. Fax: +39 010 353 8733. E-mail: alma@chimica.unige.it.
[†] INSTM and Università di Genova.
[‡] INSTM and Instituto dei Sistemi Complessi - CNR.
[§] Dipartimento di Chimica, Università di Firenze.
[||] INSTM and Dipartimento di Chimica, Università di Firenze.

10.1021/jp905787h CCC: $40.75 © 2009 American Chemical Society
Published on Web 10/20/2009

- Raman spectroscopy: SERS effect[24] is active also at 800−1000 nm, that is in a spectral region where fluorescence contributions are generally rather low and the Raman signals are then well-defined, thus allowing for instance SERS-based in vivo medical tests.
- Photonics: the strong electromagnetic-field localization induced by NCs in the NIR allows the preparation of novel composite materials formed by the metallic structure and molecular adsorbates characterized by large nonlinear properties, further enhanced by the interaction with the metal.[25−27]

The combined properties of silver and gold are expected to increase the adsorption properties and the Raman activity of the nanohybrids.

Several reasons have been considered for choosing chitosan as protecting agent in the synthesis of NCs: the well-known excellent biocompatibility, biodegradability, and nontoxicity[28−32] of this polysaccharide and its successful use in delivering therapeutic drugs, proteins, and genes by intravenous, oral, and mucosal administration[33−35] that are expected to improve the biocompatibility of these nanohybrids. Chitosan has been recently used as protecting agent in the synthesis of gold nanoparticles[36−39] because of the electrostatic interaction between the free amino groups in the polymer repeat units and the negatively charged metal surface that stabilizes the structure. Moreover, gold nanoparticles embedded in chitosan have been shown to provide suitable SERS substrates.[40]

In this paper, the synthesis and characterization of chitosan-protected nanocages (Chit-NCs) with porous walls containing Au and Ag through the galvanic replacement reaction onto silver nanoparticles (NPs) stabilized with the polymer (Chit-AgNPs) and decorated with polydiacetylene chains is reported. The choice of the polydiacetylene has been dictated by the extraordinary properties exhibited by this class of polymers.[41−44] To this end the chitosan-protected nanocages were functionalized with 10,12-pentacosadiynoic acid monomer because the presence of the carboxilyc end-group favors the anchoring of the molecule onto the particle surface and the long alkyl chains stabilize the monolayer structure. The stable nanohybrids were then irradiated with UV light to induce the monomer polymerization. The comparison of the results of the photopolymerization process of these novel bimetallic nanohybrids relative to our previous data on polydiacetylene-coated silver and gold nanoparticles[45−48] is discussed.

Experimental Methods

Reagents. All chemical reagents and solvents were spectroscopic grade commercial products purchased from Lancaster and used as received. The diacetylene monomer 10,12-pentacosadiynoic acid (PCDA), the pale blue color of which indicated the presence of traces of polymer spontaneously formed, was purified prior to use through dissolution in ethanol followed by filtration on 0.20-μm PTFE syringe filter. All aqueous solutions were made with ultrahigh-purity water purified with a Milli-Q Plus ultrapure water system (Millipore Co.)

Synthetic Procedures. ***Chitosan-Protected Silver Nanoparticles (Chit-AgNPs).*** A 2% w/v solution of chitosan was obtained in acetic medium by dissolving 100 mg of the polymer in 50 mL of 1% acetic acid solution. The as-prepared chitosan solution (7.2 mL) was added to an aqueous solution of $AgNO_3$ (18 mL, 5 mM) under magnetic stirring; half an hour later, a freshly prepared aqueous solution of $NaBH_4$ (4.4 mL, 0.1 M) was added drop by drop. The solution first turned yellow, then brown, and finally became an opalescent deep yellow suspension. Stirring was maintained for ~2 h to ensure full reaction. Once obtained, the chitosan-protected AgNPs, which form stable dispersions in water without introducing additional stabilizers, were kept at room temperature.

Chitosan-Protected Nanocages (Chit-NCs). Chit-NCs in Au−Ag alloy were prepared through a galvanic replacement reaction between Chit-AgNPs and $HAuCl_4$.[16,17] In each preparation, 1.5 mL of the as-prepared Chit-AgNP suspension was dispersed in 15 mL of H_2O Milli-Q. The mixture was refluxed for 10 min under magnetic stirring before a specific volume of 20 mM $HAuCl_4$ aqueous solution was added dropwise. The suspension immediately became darker and finally turned gray-blue. Heating was maintained for another 20 min until the color became stable. The mixture was then cooled to room temperature and kept under vigorous stirring overnight. Once again, the resulting product was stored at room temperature for further treatments and TEM characterization.

PCDA-Functionalized Nanoparticles and Nanocages. As prepared, the chitosan-protected nanoparticles and nanocages were coated with PCDA molecules by adding the colloidal suspensions of a proper amount of the monomer dissolved in ethanol (Au/diacetylene molar ratio = 1:1.5). The resulting suspensions were maintained under vigorous stirring overnight to allow the reaction to complete and then purified from PCDA excess by repeated centrifugation for 30 min at 5000 rpm speed; the final precipitate was redispersed in a given volume of 0.5% w/v chitosan aqueous solution and then stored at room temperature.

Diacetylene Polymerization. The photopolymerization process was carried out directly in the aqueous suspensions in a Rayonet photochemical chamber reactor, operating at 254 nm and 35 W power. The 1-cm quartz cuvette with the diacetylene-containing colloidal suspensions were kept at 10-cm distance from the UV lamps.

Transmission Electron Microscopy. Bright-field TEM images were obtained with a Jeol electron microscope, model IEM-2010, operating at 200 kV. Specimens were prepared by evaporating a drop on a 300-mesh carbon-coated copper grid (Lacey). Qwin software V3 for digital image processing and analysis was used for the measurement of particle size employing multiple pictures from different areas.

UV−Vis Spectroscopy. Electronic absorption spectra were recorded at room temperature on a Perkin-Elmer Lambda 9 spectrophotometer using 1-cm and 1-mm path length cuvettes. Deconvoluted UV−vis spectra were obtained by fitting the experimental data with the LabCalc software from Galactic Industries Corporation (1989).

Raman Spectroscopy. Raman spectra were recorded using a Jobin-Yvon HG2S monochromator equipped with a cooled RCA-C31034A photomultiplier (514.5 nm line of Ar^+ laser and 647.1 nm line of Kr^+ laser). MicroRaman spectra were collected using a Renishaw RM2000 single grating spectrograph, coupled with a diode laser source emitting at 785 nm and sample irradiation was accomplished using a 50× microscope objective of a Leica Microscope DMLM. Proper defocusing of the 3 mW laser beam permitted to reduce from 1% to 10% the power density on the samples. The laser spot size was ca. 1−3 μm. Raman light was filtered by a double holographic Notch filters system and collected by an air-cooled CCD detector. The acquisition time for each measurement was 10 s. All spectra were calibrated with respect to a silicon wafer at 520 cm^{-1}. The quartz (Suprasil) plates were furnished by Hellma GmbH (Germany).

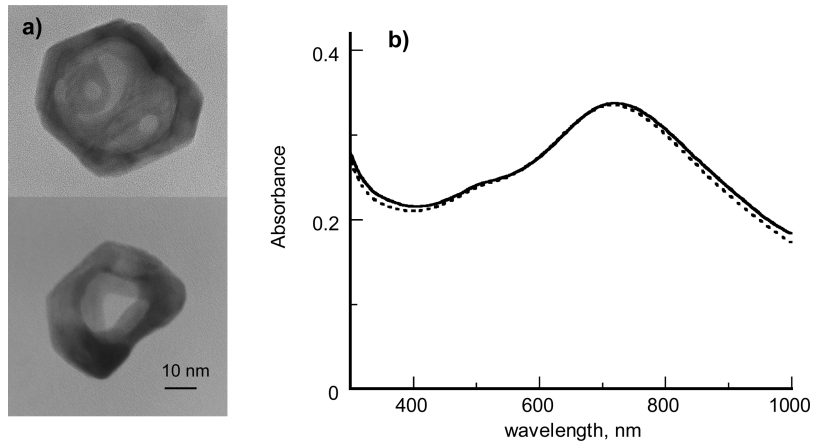

Figure 1. (a) Bright field TEM images obtained from chitosan-stabilized Au−Ag-alloyed NCs (sample 3 of Table 1). (b) Electronic absorption spectra recorded for a freshly prepared (—) and six months-aged (− − −) aqueous suspension of sample 3.

TABLE 1: Chitosan-Stabilized Nanocages: Synthesis Conditions and Morphological and Spectroscopic Properties

sample	$HAuCl_4$ concentration (mM)	Au/Ag molar ratio	mean diameter (nm)	mean thickness (nm)	λ(max) (nm)
1	0.043	0.14	49.1 ± 1.4	10.4 ± 2.6	620
2	0.050	0.16	44.0 ± 1.8	8.8 ± 1.8	700
3	0.059	0.19	44.6 ± 2.8	7.7 ± 2.5	713
4	0.062	0.20	39.4 ± 1.0	8.0 ± 2.1	710
5	0.065	0.21	35.1 ± 0.6	8.1 ± 1.9	712

Results and Discussion

The template−Ag solid nanostructures were previously obtained through a wet chemical reduction of silver nitrate using the standard method described in details in the Experimental Methods. To modulate the geometrical properties of the nanocages, the transmetalation process was carried out directly in aqueous suspension by titrating a fixed amount of Chit-AgNPs with different volumes of $HAuCl_4$ solution, according to the procedure described in ref 17. The obtained NCs were morphologically and spectroscopically investigated by TEM technique and UV−vis spectroscopy. The experimental conditions employed in the synthesis are reported in Table 1 together with the average structural and optical properties of the resulting products. As an example, the TEM images obtained from sample 3 are shown in Figure 1 together with the corresponding UV−vis spectra. It is evident that we succeeded in obtaining nanostructures with truncated corners, hollow interiors, and quite uniform and homogeneous walls, in agreement with the reaction mechanism proposed by Sun and co-workers.[17] As expected, a significant absorption band in the NIR region peaked around 700 nm, due to the surface plasmon resonance effect, is observed. The nanocage aqueous suspensions are stable, as confirmed by the unaltered profile of the electronic absorption spectrum also after six months of aging.

The data in Table 1 indicate that by increasing the Au/Ag molar ratio the morphological characteristics of nanocages vary though not regularly. In fact, whereas the mean external diameter generally decreases, a correlation between gold amount and average thickness is found only for samples 1−3. Addition of more $HAuCl_4$ does not significantly affect the wall dimensions (cf. samples 4 and 5). A similar behavior is observed for the corresponding SPR bands at longer wavelengths, the maximum of which is progressively red-shifted from 620 nm to around 710 nm and then remains unchanged. By further increasing the $HAuCl_4$ concentration, the nanocages collapse into irregularly shaped gold fragments characterized by a plasmon band centered at about 520 nm, typical of solid Au nanostructures (data not shown).

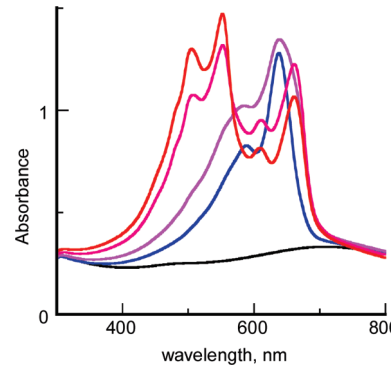

Figure 2. Electronic absorption spectra evolution with UV light (254 nm) exposure for PCDA diacetylene chemisorbed onto Au−Ag-alloyed NCs (sample 2) in water. Irradiation time (min): 0 (black), 2 (blue), 5 (purple), 60 (magenta), and 120 (red).

On the basis of these results, sample 3 was selected for functionalization with ligand chains carrying end-groups able to firmly anchor the metal surfaces. Due to the outstanding properties of polydiacetylenes (PDAs) in photonic and sensor devices, we prepared diacetylene-coated nanocages by chemisorption onto the preformed Chit-NCs of the monomer 10,12-pentacosadiynoic acid ($CH_3-(CH_2)_{11}-C\equiv C-C\equiv C-(CH_2)_8-COOH$, PCDA), following the procedure described in the Experimental Methods. Clear gray-blue colloidal suspensions of PCDA-capped NCs were obtained, stable for months in chitosan aqueous solution if properly kept in the dark. By exposing the suspension to UV light for monomer polymerization, progressive changes first to deep-blue, then to purple, and finally to pink are instead observed. The irradiation-induced color tuning, due to the photopolymerization process of the diacetylene outer-shell of the nanostructures, is described by the time dependence of the electronic absorption spectrum reported in Figure 2. At low UV exposure (2 or 5 min) the appearance of a sharp exciton band peaked at 640 nm followed by its first vibrational sideband around 590 nm indicates the presence of the polymer in the blue form. By increasing the irradiation time, the blue PDA bands shift toward higher wavelengths (around 665 and 615 nm, respectively), attributable to the more delocalized bluish-green phase.[45] In the meantime, the absorptions of the red polydiacetylene form at 555 and 505 nm become

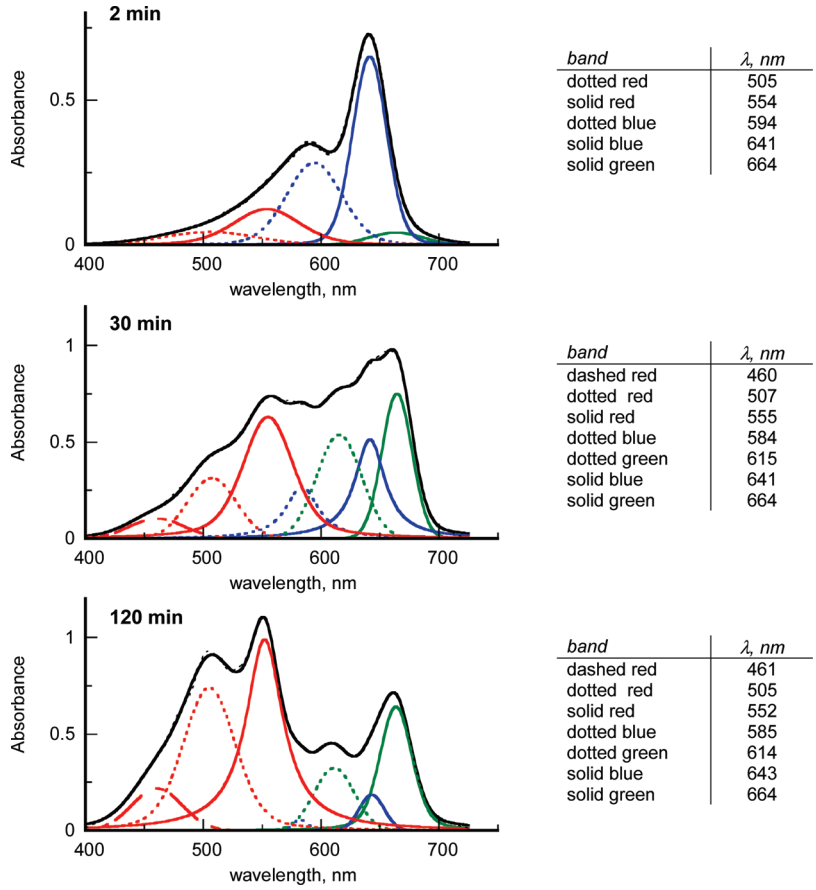

Figure 3. Deconvolution spectra of Figure 2 for three different intervals of UV exposure. The black line is obtained by adding the absorptions of the colored bands, the maximum of which is listed in the tables alongside.

discernible. At prolonged light exposure, the red bands are predominant though the contribution of the longer wavelength absorptions is not negligible.

We stress at this point that an high monomer-to-polymer conversion is observed in these systems as already found for PCDA-decorated silver nanoparticles with chitosan used as protecting agent.[48] The enhanced photopolymerization is attributable to the fundamental role played by the polysaccharide in providing the suspension homogeneity and stability most likely because of its capability of enabling electrostatic interactions with the negatively charged carboxylic end-groups of the diacetylene. This hypothesis is confirmed by the fact that PCDA-functionalized silver nanoparticles dispersed in aqueous solution containing citrate as stabilizer show at the same monomer concentration a monomer to polymer conversion about 1 order of magnitude lower, as reported in the Supporting Information section.

For a better understanding of the photoinduced polymer chromism, a deconvolution technique has been applied to the absorption spectra. The results are described in Figure 3 for three different irradiation times. The following remarks can be made. (a) At the initial stages of polymerization, the blue phase is clearly the predominant one, but the other two PDA forms (red and bluish-green) are also present, although not clearly visible in Figure 2 with the naked eye; (b) at intermediate irradiation times, the contributions of the three phases are comparable, as confirmed by the profile of the resulting spectrum; (c) at prolonged exposure, the red and the bluish-green phases prevail over the blue one, though its contribution cannot be disregarded; and (d) to account for the experimental data, a weak absorption centered at 461 nm must be considered

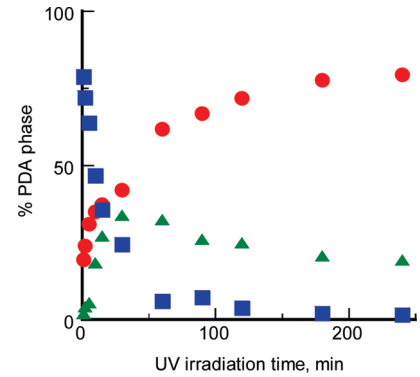

Figure 4. Time-dependence contributions of the PDA phases evaluated from the area of the Figure 3 bands. Red phase (circles), blue phase (squares), bluish-green phase (triangles).

TABLE 2: Band Assignment from the Deconvoluted Electronic Absorption Spectra of Figure 3[a]

band	exciton (nm)	first vibronic (nm)	second vibronic (nm)
PDA red phase	554	505	461
PDA blue phase	641	592	–
PDA bluish-green phase	664	612	–

[a] Peak positions are reported with an error of ± 1 nm.

at increasing irradiation time. This band could be attributed either to the second vibrational replica of the red form[49] or to the exciton of the highly undelocalized yellow phase, typical of PDA dispersed in thermodynamically good solvents.[50,51]

The complete assignment of the wavelengths corresponding to the different PDA forms, derived from a detailed analysis of

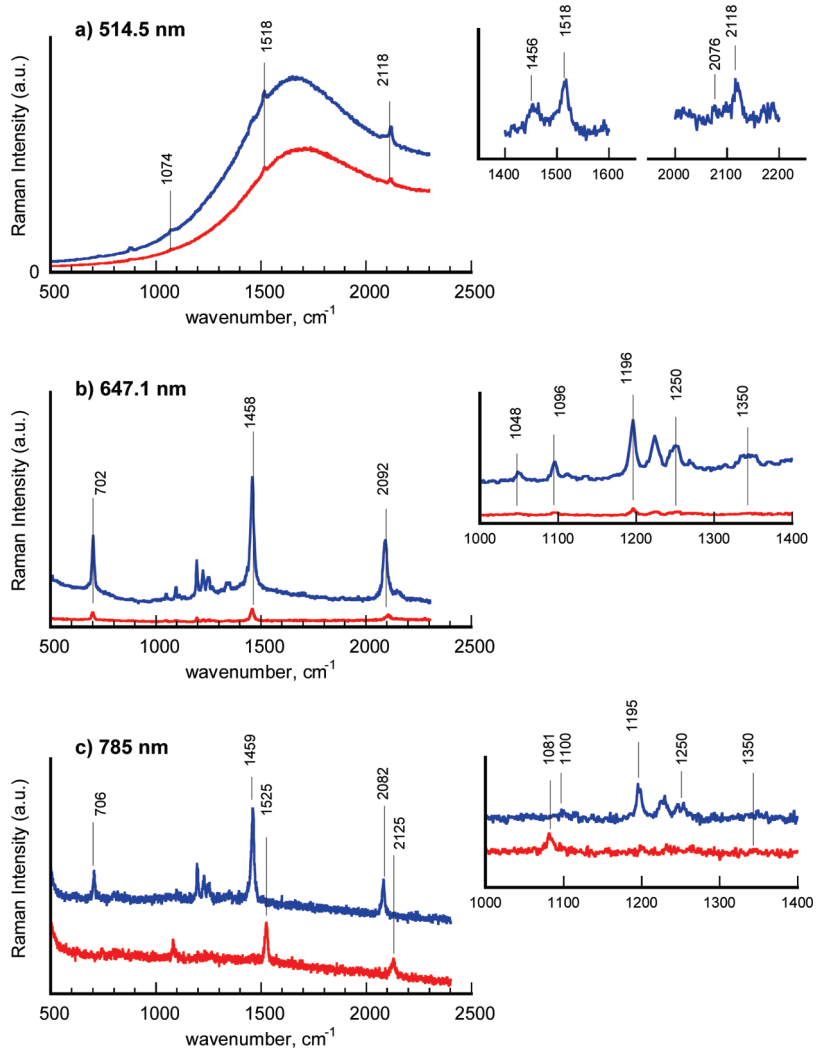

Figure 5. Raman spectra recorded at three different laser light excitation for PCDA-coated NCs subjected to UV light for 2 (blue line) and 60 (red line) min. (a) 514.5 nm-laser excitation: Raman spectra of the aqueous suspension; inset: difference spectra with respect to the fluorescence background for the 2-min irradiated sample. (b) 647.1 nm-laser excitation: Raman spectra of the aqueous suspension; inset: magnification of the Raman spectra in the 1000−1400-cm^{-1} spectral region. (c) 785 nm-laser excitation: Raman spectra of the irradiated PCDA-coated NCs after deposition onto quartz substrates; inset: magnification of the Raman spectra in the 1000−1400-cm^{-1} spectral region.

the deconvoluted spectra, is reported in Table 2. The time-dependence of the contributions of the different phases, evaluated from the area of each band, is reported in Figure 4. By comparing the data of Table 2 with those reported in a previous paper for the same polydiacetylene chemisorbed onto silver nanoparticles (AgNPs) of comparable size,[45] various differences in the photopolymerization process can be observed. In fact, while the blue band is positioned at the same wavelength (641 nm), the absorptions of the other two phases are blue-shifted: 554 nm instead of 560 nm for the red band and 664 nm instead of 671 nm for the bluish-green one. This finding is particularly relevant for the highly conjugated chain because it suggests that the unusual bluish-green PDA phase can be formed onto the hollow porous nanostructures only with a reduced electronic delocalization. The bluish-green phase is always a minority form for polyPCDA onto NCs (Figure 4), while it is the predominant one at long irradiation times when the polymer is self-assembled onto the solid counterparts.[45]

Further information on the photopolymerization process of PCDA-coated NCs was obtained by Raman technique. The present results can be interpreted using the assignment previously proposed for the same polymer on silver nanoparticles: the wavenumbers corresponding to the triple, double and single CC bond stretching modes of the PDA different forms, respectively, change from 2073, 1448, and 1096 cm^{-1} for the bluish-green phase to 2080, 1484, and 1082 cm^{-1} for the blue and to 2115, 1513, and 1070 cm^{-1} for the red one. The Raman spectra recorded for the NCs colloidal suspensions by exciting at 514.5 and 647.1 nm at two different irradiation times (2 and 60 min) are reported in Figure 5a and b. The Raman spectrum corresponding to excitation at 514.5 nm shows only very weak features on top of the fluorescence background related to the red phase. By subtracting this band, the peaks associated with the triple and double CC bond stretching modes of the bluish-green (2076 and 1456 cm^{-1}) and red (2118 and 1518 cm^{-1}) forms are observed for the spectrum at 2 min irradiation time (inset of Figure 5a). For prolonged UV exposure, only signals typical of the red phase are evident. A well-defined spectrum is observed with the 647.1 nm exciting line, in resonance with the nonfluorescent blue and bluish-green forms. The two peaks at 1458 cm^{-1}, typical of the bluish-green structure, and at 2092 cm^{-1}, associated with the blue polymer, show the coexistence of both phases that are present also after 60 min irradiation. More insights were obtained from the Raman spectra at 785 nm of PCDA-coated NCs deposited on quartz substrate (Figure 5c). Signals typical of the resonant bluish-green structure (2082

TABLE 3: Band Assignment from the Raman Spectra of Figure 5[a]

laser excitation (nm)	peak position (cm^{-1})	mode assignment	peak assignment
514.5	1074	C−C stretching	PDA red phase
	1456	C═C stretching	PDA bluish-green phase
	1518	C═C stretching	PDA red phase
	2076	C≡C stretching	PDA bluish-green phase
	2118	C≡C stretching	PDA red phase
647.1	702	C−C−C in-plane bending	PDA bluish-green phase
	1048	C−C stretching	backbone gauche conformation
	1096	C−C stretching	backbone gauche conformation
	1196	CH_2 wagging	$(CH_2)_8COO^-$ group
	1250	CH_2 wagging	$(CH_2)_8COO^-$ group
	1350	CH_2 wagging	$(CH_2)_{11}CH_3$ group
	1458	C═C stretching	PDA bluish-green phase
	2092	C≡C stretching	PDA bluish-green phase
785	706	C−C−C in-plane bending	PDA bluish-green phase
	1081	C−C stretching	PDA red phase
	1100	C−C stretching	PDA bluish-green phase
	1195	CH_2 wagging	$(CH_2)_8COO^-$ group
	1250	CH_2 wagging	$(CH_2)_8COO^-$ group
	1350	CH_2 wagging	$(CH_2)_{11}CH_3$ group
	1459	C═C stretching	PDA bluish-green phase
	1525	C═C stretching	PDA red phase
	2082	C≡C stretching	PDA bluish-green phase
	2125	C≡C stretching	PDA red phase

[a] Peak positions are reported with an error of ±4 cm^{-1} for the Raman spectra obtained by 514.5 nm and 647.1 nm laser excitations. MicroRaman measurements are performed by 785 nm laser excitation with an error of ±1 cm^{-1}.

and 1459 cm^{-1}) are observed for short irradiation. Afterward, only peaks of the red form are present. The small increase in the wavenumbers of the bluish-green form with respect to those in ref 45 is in agreement with the observation previously made of a reduced electronic delocalization degree of this phase on hollow porous nanostructures. Information on the conformational properties of the alkylic groups is derived from the insets of Figure 5b and c, where peaks at 1195, 1250 cm^{-1} and a weak feature at about 1350 cm^{-1} (Table 3) are observed. These signals, previously detected for the bluish-green phase of polyPCDA self-assembled onto AgNPs and assigned to wagging modes of methylene units in all-trans conformation,[45] indicate that a compact organization of the chemisorbed ligands is formed also in nanocages, favoring a backbone delocalization more extended than that typical of the blue phase.

It is worth noting that these novel nanostructures allow detection of very well-defined bands assigned only to the various chromatic polydiacetylene forms. No signal arising from chitosan modes is present, as instead observed in the SERS of Au−chitosan films dipped in R6G solution.[40] We believe SERS and surface-enhanced resonance Raman scattering (SERRS)[52] effects to be responsible for the intensity enhancement of the polyPCDA Raman modes.

Conclusions

The results here presented provide insights into the fundamental properties of PCDA-coated chitosan-stabilized nanocages that have allowed to control the optical response of the photogenerated polydiacetylene. The nanocages were synthesized through galvanic replacement reaction between the chitosan-protected silver nanoparticles and $HAuCl_4$ in aqueous suspension followed by chemisorption of the diacetylene monomers onto the metal surface of the as-prepared hollow nanostructures. The role played by chitosan was found to be determinant in enhancing the photopolymerization yield, as well as in conferring stability and biocompatibility to the system. The formation of compact structures of the polymer, as shown by the presence of all-trans configuration of the alkylic chains, favors the PDA bluish-green phase similarly to what previously observed in silver nanoparticles coated with the same monomer. Although the structure of the bluish-green form is still under debate, these novel composite materials, combining the extraordinary optical nonlinear properties of the polydiacetylene chain and the electromagnetic-field enhancing capability of metal nanocages in the near-infrared, are expected to show improved response in the telecommunication field or in the high-resolution imaging for sensing applications.

Moreover, because of their stability and reproducibility, as well as the possibility of obtaining SERS spectra with a variety of excitation lines from the vis to the NIR, the chitosan-decorated nanocages represent also suitable solution for SERS substrates.

Acknowledgment. Financial support from PRIN 2007 "Plasmonic nanostructures and their interaction with chromophores: towards innovative photonic devices and optical sensors" (Contract No. 2007LN873M) and from PRIN 2007 "Organic materials for photovoltaic and electroluminescent devices: design, synthesis, evaluation" (Contract No. 2007PBWN44) are acknowledged.

Supporting Information Available: Figure showing the electronic absorption spectrum of 1-min irradiated PCDA-decorated AgNPs in chitosan-containing and citrate-containing aqueous suspensions. This material is available free of charge via the Internet at http://pubs.acs.org.

References and Notes

(1) Rao, C. N. R.; Müller, A.; Cheetham, A. K. *The chemistry of nanoparticles: synthesis, properties and applications*; Wiley-VCH: Weinheim, 2004.
(2) Vayssieres, L.; A. Manthiram, A. *Encyclopedia of Nanoscience and Nanotechnology*; Nalwa, H. S., Ed.; American Scientific: Steveson Ranch, CA, 2004; p 147.
(3) Sounart, T. L.; Liu, J.; Voigh, J. A.; Hsu, T. W. P.; Spoerke, E. D.; Tian, Z. R.; Jiang, Y. B. *Adv. Funct. Mater.* **2006**, *16*, 335.
(4) Prodan, E.; Nordlander, P. *Nano Lett.* **2003**, *3*, 543.
(5) Prodan, E.; Nordlander, P. *J. Chem. Phys.* **2004**, *120*, 5444.
(6) Kottmann, J. P.; Martin, O. J. F.; Smith, D. R.; Schultz, S. *Phys. Rev. B* **2001**, *64*, 235402.
(7) Sershen, S. R.; Westcott, S. L.; Halas, N. J.; West, J. L. *Appl. Phys. Lett.* **2002**, *80*, 4609.
(8) Jackson, J. B.; Westcott, S. L.; Hirsch, L. R.; West, J. L.; Halas, N. J. *Appl. Phys. Lett.* **2003**, *82*, 257.
(9) Murphy, C. J.; Jana, N. R. *Adv. Mater.* **2002**, *14*, 80.
(10) Kim, F.; Song, J. H.; Yang, P. J. *J. Am. Chem. Soc.* **2002**, *124*, 14316.
(11) Poshusta, J. C.; Tuan, V. A.; Pape, E. A.; Noble, R. D.; Falconer, J. L. *AlChE J.* **2000**, *46*, 779.
(12) Li, S.; Falconer, J. L.; Noble, R. D. *J. Membr. Sci.* **2004**, *241*, 121.
(13) Cui, Y.; Kita, H.; Okamoto, K.-I. *J. Mater. Chem.* **2004**, *14*, 924.
(14) Li, S.; Martinek, J. G.; Falconer, J. L.; Noble, R. D. *Ing. Eng. Chem. Res.* **2005**, *44*, 3220.
(15) Li, S.; Alvarado, G.; Falconer, J. L.; Noble, R. D. *J. Membr. Sci.* **2005**, *251*, 59.
(16) Sun, Y.; Mayers, B. T.; Xia, Y. *Nano Lett.* **2002**, *2*, 481.
(17) Sun, Y.; Xia, Y. *J. Am. Chem. Soc.* **2004**, *126*, 3892.
(18) Liang, H.; Guo, Y.; Zhang, H.; Hu, J.; Wan, J.; Bai, C. L. *Chem. Commun.* **2004**, 1496.
(19) Liang, H. P.; Wan, L. J.; Bai, C. L.; Jiang, L. *J. Phys. Chem. B* **2005**, *109*, 7795.

(20) Shukla, S.; Priscilla, A.; Banerjee, M.; Bionde, R. R.; Ghatak, J.; Satyam, P. V.; Sastry, M. *Chem. Mater.* **2005**, *17*, 5000.
(21) Selvakannan, P. R.; Sastry, M. *Chem. Commun.* **2005**, 1684.
(22) Sun, Y.; Xia, Y. *Nano Lett.* **2003**, *3*, 1569.
(23) Chen, J.; Saeki, F.; Wiley, B. J.; Cang, H.; Cobb, M. J.; Li, Z.-Y.; Au, L.; Zhang, H.; Kimmey, M. B.; Li, X.; Xia, Y. *Nano Lett.* **2005**, *5*, 473.
(24) *Surface-Enhanced Raman Scattering: Physics and Applications*; Kneipp, K., Moskovits, M., Kneipp, H., Eds.; Springer-Verlag: Berlin, Heiderlberg, 2006.
(25) Giorgetti, E.; Margheri, G.; Sottini, S.; Toci, G.; Muniz-Miranda, M.; Moroni, L.; Dellepiane, G. *Phys. Chem. Chem. Phys.* **2002**, *4*, 2762.
(26) Wenseleers, W.; Stellacci, F.; Meyer-Friedrichsen, T.; Mangel, T.; Bauer, C. A.; Pond, S. J. K.; Marder, S. R.; Perry, J. W. *J. Phys. Chem. B* **2002**, *106*, 6853, and references therein.
(27) Zeng, X. C.; Bergman, D. J.; Hui, P. M.; Stroud, D. *Phys. Rev. B* **1988**, *38*, 10970.
(28) Dufresnea, A.; Cavaillea, J. Y.; Dupeyea, D.; Ramirez, M. G.; Romeroc, J. *Polymer* **1999**, *40*, 1657.
(29) Kweon, H. Y.; Um, I. C.; Park, Y. H. *Polymer* **2001**, *42*, 6651.
(30) Fuentes, S.; Retuert, P. J.; Ubilla, A.; Fernandez, J.; Gonzalez, G. *Biomacromolecules* **2000**, *1*, 239.
(31) Tanabe, T.; Okitsu, N.; Tachibana, A.; Yamauchi, K. *Biomaterials* **2002**, *23*, 817.
(32) Zhang, M.; Li, X. H.; Gong, Y. D.; Zhao, N. M.; Zhang, X. F. *Biomaterials* **2002**, *23*, 2641.
(33) Janes, K. A.; Calvo, P.; Alonso, M. J. *Adv. Drug Delivery Rev.* **2001**, *47*, 83.
(34) Mao, H.-Q.; Roy, K.; Troung-Le, V. L.; Janes, K. A.; Lin, K. Y.; Wang, Y.; August, J. T.; Leong, K. W. *J. Controlled Release* **2001**, *70*, 399.
(35) Remunan-Lopez, C.; Vila-Jato, J. L.; Alonso, M. J.; Calvo, P. *J. Appl. Polym. Sci.* **1997**, *63*, 125.
(36) Esumi, K.; Takei, N.; Yoshimura, T. *Colloids Surf., A* **2001**, *182*, 239.
(37) Huang, H.; Yuan, Q.; Yang, X. *J. Colloid Interface Sci.* **2005**, *282*, 26.
(38) Sugunan, A.; Thanachayanont, C.; Dutta, J.; Hilborn, J. G. *Sci. Technol. Adv. Mater.* **2005**, *6*, 335.
(39) Caseli, L.; dos Santos, D. S.; Aroca, R. F.; Oliveira, O. N. *Mater. Sci. Eng., C* **2009**, *29*, 1687.
(40) dos Santos, D. S.; Goulet, P. J. G.; Pieczonka, N. P. W.; Oliveira, O. N.; Aroca, R. F. *Langmuir* **2004**, *20*, 10273.
(41) Batchelder, D. N.; Evans, S. D.; Freeman, T. L.; Häussling, L.; Ringsdorf, H.; Wolf, H. *J. Am. Chem. Soc.* **1994**, *116*, 1050.
(42) Kim, T.; Chan, K. C.; Crooks, R. M. *J. Am. Chem. Soc.* **1997**, *117*, 3963, and references therein.
(43) Menzel, H.; Mowery, M. D.; Cai, M.; Evans, C. E. *Macromolecules* **1999**, *32*, 4343, and references therein.
(44) Cai, M.; Mowery, M. D.; Pemberton, J.; Evans, C. E. *Appl. Spectrosc.* **2000**, *54*, 31.
(45) Raimondo, C.; Alloisio, M.; Demartini, A.; Cuniberti, C.; Dellepiane, G.; Jadhav, S. A.; Petrillo, G.; Giorgetti, E.; Gellini, C.; Muniz-Miranda, M. *J. Raman Spectroscopy*, **2009**, doi 10.1002/jrs.2327.
(46) Alloisio, M.; Demartini, A.; Cuniberti, C.; Muniz-Miranda, M.; Giorgetti, E.; Giusti, A.; Dellepiane, G. *Phys. Chem. Chem. Phys.* **2008**, *10*, 2214.
(47) Alloisio, M.; Demartini, A.; Cuniberti, C.; Dellepiane, G.; Muniz-Miranda, M.; Giorgetti, E. *Vibrational Spectrosc.* **2008**, *48*, 53.
(48) Alloisio, M.; Demartini, A.; Cuniberti, C.; Dellepiane, G., paper presented at E-MRS Spring Meeting 2009, Strasbourg, France and submitted to *Sensor Letters*.
(49) Alloisio, M.; Cravino, A.; Moggio, I.; Comoretto, D.; Bernocco, S.; Cuniberti, C.; Dell'Erba, C.; Dellepiane, G. *J. Chem. Soc., Perkin Trans 2* **2001**, 146.
(50) Ye, Q.; Zou, G.; You, X.; Yu, X.; Zhang, Q. *Mater. Lett.* **2008**, *62*, 4025.
(51) Zuilhof, H.; Barentsen, H. M.; Van Dijk, M.; Sudhölter, E. J. R.; Hoofman, R. J. O. M.; Siebbeles, L. D. A.; de Haas, M. P.; Warman, J. M. *Supramolecular Photosensitive and Electroactive Materials*; Nalwa, H. S., Ed.; Academic Press: New York, 2001; Chapter *4*.
(52) Piczonka, N. P. W.; Goulet, P. J. G.; Aroca, R. F. *Surface-Enhanced Raman Scattering: Physics and Applications*; Kneipp, K., Moskovits, M., Kneipp, H., Eds.; Springer-Verlag: Berlin, Heidelberg, 2006; pp 197−216.

JP905787H